

Transferability of bulk empirical potentials to silicon microclusters: A critical study

Wanda Andreoni and Giorgio Pastore*

IBM Research Division, Zurich Research Laboratory, 8803 Rüschlikon, Switzerland

(Received 25 January 1990)

We explore in detail the “transferability” of classical bulk-derived potentials to microclusters, in the case of silicon. We present a critical comparison of the results of our computer simulations performed both with the local-density-functional (LDF) Car-Parrinello method and with published potentials obtained from fitting to LDF calculations of bulk properties. We show quantitatively that classical potentials give only a poor description of the potential-energy surface of the microclusters. For the latter we provide much of the information needed to construct an improved classical scheme.

Simulating the growth process of real materials is an ambitious goal of computational solid-state physics.¹ For this, it would be highly desirable to have an accurate empirical scheme based on an interatomic potential that was capable of reproducing, e.g., the structural and thermal properties of the infinite solid and at the same time those of small atomic clusters. A large effort has recently been made to construct empirical potentials for silicon,^{2–9} starting however from a data base which is largely limited to *bulk* properties.¹⁰ With such an approach, the immediate question is whether, in view of the highly different chemical bonding, such bulk-derived potentials are “transferable” to the realm of small aggregates. Several applications of bulk empirical potentials to silicon microclusters have recently appeared,^{7–9,11,12} however, with only a very limited comparison with results of quantum-mechanical calculations. We believe it is important that an extensive and accurate comparison of this type now be carried out.

In the absence of experimental data for the microclusters, the only consistent way to investigate the issue of the “transferability” of the potentials is within one well-defined theoretical framework. This is offered by the local-density-functional–pseudopotential (LDA-P) scheme. We have performed simulated annealing and finite-temperature simulations of silicon microclusters with both (i) the direct LDA-P molecular dynamics (Car-Parrinello) method,^{13,14} and (ii) the Tersoff³ and Chelikowsky *et al.*⁷ potentials, which were derived from fitting to the LDA-P results for the bulk solid in several structures with different coordination. We shall refer to these potentials as *P1* and *P2*, respectively. In particular, we shall discuss here in detail the predicted low-energy structures and some characteristics of the potential-energy surfaces for aggregates of up to ten atoms, and in this way give a *quantitative* demonstration that the agreement between (i) and (ii) is rather poor.

First we consider the lowest-energy structures found (via simulated annealing strategies) for Si_N ($N=4-10$) with the above potentials and LDA.¹⁵ In the case of Si_6 , two quasidegenerate isomers ($\Delta E \sim 0.01$ eV/atom) have been found in LDA [a distorted trigonal bipyramid (dTBP) + 1 cap (1C) and an octahedron (O)]. We point

out that the predictions for ground-state structures obtained with all-electron configuration interaction (CI) methods^{16,17} agree with our results, with the exception of Si_9 . In this case, however, the discrepancy may be due to the fact that the set of atomic configurations considered in the CI calculations in the search for the minimum energy did not include our lowest-energy structure (which is the result of a more efficient optimization procedure). Instead, notable discrepancies exist with the simulated-annealing results of the empirical potentials. These fail for $N=4$ (tetrahedron instead of rhombus), predict the correct topologies for $N=5-7$ [TBP, octahedron, pentagonal bipyramid (PBP)], and again give different topologies for $N=8-10$ (see below). We note that for $N=4-7$, the three-body potentials actually predict the same structures that a Lennard-Jones (LJ) potential would—structures which correspond to optimizing the compactness of spheres. Silicon atoms apparently behave like spheres in this respect for $N=5-7$, but the optimization of the chemical bonding “requirements” strongly affects this behavior for the tetramer and subtly modifies it for $N \geq 8$.

The “bond network” found with the empirical potentials is not “similar” to that predicted by LDA. This can be seen by comparing, e.g., the average coordination number (CN) [see Fig. 1(a)] which corresponds to the appropriate cutoff distance R_c in each case ($R_c = 5.0$ a.u. for LDA and *P1*, $R_c = 5.3$ for *P2* where the minimum bond length is ~ 0.3 a.u. larger).¹⁸ This is illustrated in Fig. 1(a) for $N=4-10$. Structures with the same topology do not necessarily have the same CN. This is due to the definition of a cutoff and to the distortions (from the regular polyhedra) which may be different in the different schemes. We note that the same definition of the cutoff distance is appropriate for LDA and CI results and that the CN's are also the same.

Figure 1(b) shows the behavior of the bond length with increasing size and, more specifically, that of the ratio between the average bond length of the aggregates and the bulk bond length. In the *P2* potential scheme, the size dependence manifests itself as a bond length increase with decreasing size: This behavior is known to be correct in the case of rare gases, but is not physical for silicon. Moreover, this potential predicts values of ~ 5 a.u. for

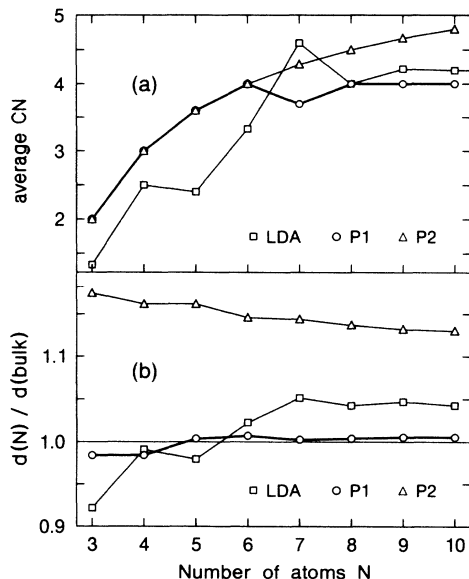


FIG. 1. Size dependence of (a) average coordination number and (b) average bond length referred to the bulk value. For Si_6 , the values refer to the edge-capped trigonal bipyramid.

Si-Si bonds, which is too large. We have calculated that such a stretch typically costs a microcluster in a given structure an energy of about 0.5 eV per pair of atoms. In the case of the $P1$ potential, instead, the variation with size goes in the expected direction and decreases with decreasing CN. We notice, however, that for $N \geq 6$, the bond length remains essentially unchanged, consistent with the fact that this potential predicts invariably a CN of 4 [see Fig. 1(a)].

To appreciate the differences between the various predictions better, we have examined the energy ordering of different local minima. This is obviously critical for the

assessment of the quality of a model potential. In Table I we report the energy ordering of topologically different structures for Si_8 , Si_9 , and Si_{10} . For this comparison we have fully relaxed the individual geometries in each scheme. We explicitly indicate the cases where one specific geometry does not correspond to a local minimum, but simply collapses to a different one. It is clear that the structural energy ordering predicted by LDA is not reproduced at all by the empirical potentials. In fact, in both the $P1$ and $P2$ schemes, the structures which are lower on the LDA energy surface are invariably found a few eV higher than the corresponding ground states. Vice versa, in most cases, the latter do not even correspond to local minima in the LDA calculations. Interestingly, however, the crystal fragments are highly unstable in both $P1$ and $P2$ schemes, in agreement with *ab initio* results and in contrast with the findings of another LDA-derived potential.⁴

In the case of the eight-atom cluster, geometries resulting from capping of (distorted) octahedra (dO) [in either trans (t) or skewed (sk) positions] are highly favored over the antiprism (AP) and the Bernal structure predicted by the $P1$ and $P2$ potentials, respectively. Interestingly, the Bernal structure¹⁹ (also described as dodecadeltahedron or tetrahemihedron²⁰) corresponds to the optimum arrangement for spheres as demonstrated by Werfelmeier long ago.²¹ We have also considered the isomer resulting from capping a pentagonal bipyramid, which corresponds to the ground state for LJ systems.²⁰ This is relatively low in energy (0.07 eV/atom) in LDA, and higher in both potential schemes. Indeed, in the case of the $P1$ potential the distortion is so large that it is only barely classifiable as a PBP+1 (the distortion is such that it gives a CN of 4 instead of 4.6). In the case of Si_9 , LDA predicts the pentagonal "motif" as the most stable one [Bernal (B)+1C, PBP+2C], in contrast to the potentials which favor the distorted [elongated (e) or squashed (s)] trigonal prisms (TP) with three caps. Also, capping of the octahedron re-

TABLE I. Structural energy ordering (ΔE in eV).

	Si_8					
	dO+2tC	dO+2skC	dPBP+1	AP	Bernal	
LDA	0	0.36	0.58	2.08	not min	
$P1$	2.58	not min	0.87 ^a	0	1.3	
$P2$	1.81	not min	1.31	not min	0	
	Si_9					
	B+1C	PBP+2C	dO+3C	AP+1C	eTP+3C	sTP+3C
LDA	0	0.49	1.10	2.20	not min	not min
$P1$	2.22	0.40	4.47	0.81	0	1.45
$P2$	2.02	0.90	4.37	not min	not min	0
	Si_{10}					
	dTP+4C	dO+4C	BA	dBA ^a		
LDA	0	0.65	not min	not min		
$P1$	2.68	6.1	not min	0		
$P2$	1.60	6.7	0	not min		

^aStrong distortion (see text).

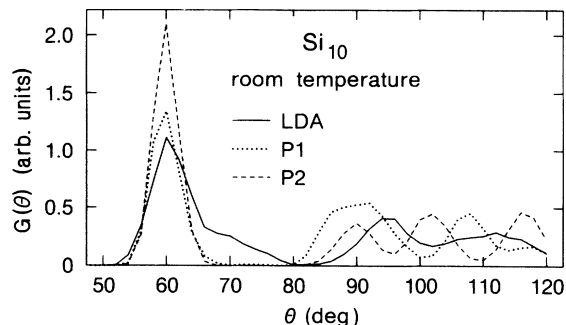


FIG. 2. Si_{10} : bond-angle distribution at room temperature.

sults in relatively low-energy structures in LDA (in agreement with CI calculations) and in high-energy configurations in both potential schemes. The geometries in Table I for the ten-atom cluster are the (distorted) trigonal prism (dTP) with 4C, the octahedron with 4C, the bi-capped antiprism (BA), and a “distorted” version which corresponds to the lowest-energy structure for the $P1$ potential. The former two, which are low and rather close in energy in both LDA and CI schemes, are local minima in the classical potentials but at high energy and with a large energy difference. The BA, which is the ground state also for the LDA-derived potential in Ref. 4, is regular in a classical potential scheme and corresponds to a high optimization of compactness for spheres [see the relatively high CN in Fig. 1(a)]. In LDA it acquires a tetragonal distortion, which decreases the average CN, and corresponds to a saddle point (located on a very flat region of the potential-energy surface). This relaxes spontaneously to the ground state. In the case of the $P1$ potential, this structure is also on a flat portion of the potential-energy surface but prefers to distort in such a way that each atom acquires fourfold coordination.

In general, the $P1$ -potential-energy surface seems to be rather flat around the local minima, with distorted arrangements favored over ordered ones: This is the case, for instance, for Si_7 , where the largely distorted PBP is favored over the ordered one, which is higher by ~ 0.21 eV (0.03 eV/atom). In the LDA such a distortion does not correspond either to a minimum or a saddle point and costs the system about 2 eV. In the case of Si_{11} , instead, the LDA potential-energy surface is rather flat, in the sense that at least four structures are found within 0.1 eV/atom. This is not the case for the prediction of the empirical potentials, which tend to magnify the structural energy differences. Discrepancies in morphologies and CN's persist at the largest cluster we have calculated with

TABLE II. Structural parameters of Si_{10} at room temperature.

	R (a.u.)	η	$\alpha_{>}$ (%)
LDA	4.23	0.05	49
$P1$	4.11	0.25	60
$P2$	4.39	0.34	48

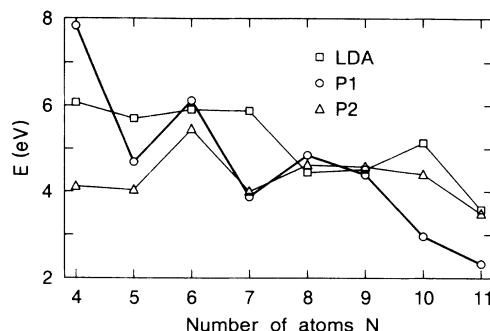


FIG. 3. Size dependence of the fragmentation energy $E = E(N) - E(N-M) - E(M)$, M being the most favorable channel.

high accuracy using the Car-Parrinello method, i.e., $N=16$.²² We stress that the previously published results for the $T=0$ equilibrium structures obtained with other classical silicon potentials point to similar^{4,8,9} or even larger¹¹ disagreement with quantum-mechanical calculations.

In spite of the fact that the location of the local minima is not well represented by the empirical potentials, one could hope that the energy barriers from one to the next might be very low and that at room temperature the similarity between the predictions would be greater. This, however, is not the case, since excitations at room temperature are not sufficient to change the topology of the potential-energy surface significantly. We have examined this point explicitly by performing finite-temperature simulations and looking for possible structural changes with temperature. An example is in Fig. 2, which shows the bond angle distribution function of Si_{10} at room temperature in the three schemes. In all cases, they correspond to the broadening of that of the ground state, and are remarkably different. In Table II we report the values of three structural parameters at room temperature for Si_{10} : The eccentricity η (defined in terms of the moments of inertia), the average radius of the cluster, and the percentage $\alpha_{>}$ of angles larger than 80° .

Finally, in Fig. 3 we report what each scheme predicts for the size dependence of the fragmentation energy corresponding to the most favorable dissociation channel. This is given in Table III, together with other channels in a

TABLE III. Predictions for the most favorable dissociation channel ($M, N-M$) of the N -atom cluster (see text).

N	LDA	$P1$	$P2$
4	3+1	3+1	3+1
5	4+1	4+1	4+1
6	5+1	5+1	5+1
7	6+1	6+1	6+1
8	7+1 (4+4)	4+4	7+1
9	7+2 (5+4, 6+3)	8+1 (5+4)	8+1
10	6+4 (7+3, 5+5)	6+4	9+1
11	7+4 (6+5)	6+5	10+1

range of 0.3 eV. In the $P2$ scheme, dissociation through loss of one atom is invariably favored over the other paths by a few eV. Again we stress that both the energy trend and the prediction for the most probable fragmentation channels found with LDA are in excellent agreement with the results of CI calculations,²³ and with the experimental data on the positively charged clusters.²⁴ A clear discrepancy exists with the results of the potentials. In particular, these would predict a relatively low stability for the ten-atom silicon cluster, which corresponds to a well-defined magic number.

In conclusion, we have shown that bulk-derived poten-

tials for silicon are *not* directly transferable to small aggregates. This suggests that in constructing empirical potential schemes suitable for reproducing the behavior of covalent systems in different states of aggregation, an interesting path to follow would be to include also a range of small clusters in the initial data base. We believe that the analysis presented here will be useful for future attempts in this direction.

We thank E. Tosatti and U. Roethlisberger for useful discussions.

*Present address: International School of Advanced Studies, 34014 Trieste, Italy.

¹See, for instance, I. K. Schuller, *Mater. Res. Soc. Bull.* **13**, 23 (1988).

²F. H. Stillinger and T. A. Weber, *Phys. Rev. B* **31**, 5262 (1985).

³J. Tersoff, *Phys. Rev. B* **37**, 6991 (1988).

⁴R. Biswas and D. R. Hamann, *Phys. Rev. B* **36**, 6434 (1987).

⁵B. W. Dodson, *Phys. Rev. B* **35**, 2795 (1987).

⁶E. Kaxiras and K. C. Pandey, *Phys. Rev. B* **38**, 12736 (1988).

⁷J. R. Chelikowsky, J. C. Phillips, M. Kamal, and M. Strauss, *Phys. Rev. Lett.* **62**, 292 (1989); *ibid.* **63**, 1649 (1989).

⁸A. D. Mistryotis, N. Flytzanis, and S. C. Farantos, *Phys. Rev. B* **39**, 1212 (1989).

⁹M. I. Baskes, J. S. Nelson, and A. F. Wright, *Phys. Rev. B* **40**, 6085 (1989).

¹⁰For a critical application to vibrational properties, see E. R. Cowley, *Phys. Rev. Lett.* **60**, 2379 (1988).

¹¹E. Blaisten-Barojas and D. Levesque, *Phys. Rev. B* **34**, 3910 (1986); B. P. Feuston, R. K. Kalia, and P. Vashishta, *ibid.* **35**, 6222 (1987); **37**, 6297 (1988); G. A. Antonio, B. P. Feuston, R. K. Kalia, and P. Vashishta, *J. Chem. Phys.* **88**, 7671 (1988).

¹²J. L. Chen and C. S. Wang, *Bull. Am. Phys. Soc.* **34**, 409 (1989).

¹³R. Car and M. Parrinello, *Phys. Rev. Lett.* **55**, 2471 (1985).

¹⁴Some preliminary results using the CP method are in P. Balone, W. Andreoni, R. Car, and M. Parrinello, *Phys. Rev. Lett.* **60**, 271 (1988). The present calculations use a larger

energy cutoff for the expansion of the electron wave functions in plane waves (11 Ry) and a more accurate representation of the angular-momentum-dependent atomic pseudopotential (s , p , and d projections).

¹⁵Some results of LDA calculations for silicon microclusters are in D. Tománek and M. Schlüter, *Phys. Rev. B* **36**, 1208 (1987).

¹⁶K. Raghavachari, *J. Chem. Phys.* **84**, 5672 (1986); K. Raghavachari and C. M. Rohlfing, *ibid.* **89**, 2219 (1988).

¹⁷G. Pacchioni and J. Koutecký, *J. Chem. Phys.* **84**, 3301 (1986).

¹⁸With the exception of LDA-Si₆, this choice for R_c is unambiguous since the closest neighbors are at least 0.5 a.u. further away. In LDA-Si₆, an increase of R_c by 0.2 a.u. would change CN from 3.33 to 3.67 in the edge-capped TBP structure and from 2.67 to 4.33 in the squashed octahedron. The structural details will be published elsewhere (Ref. 22).

¹⁹J. D. Bernal, *Nature (London)* **185**, 68 (1960).

²⁰M. R. Hoare and J. A. McInnes, *Adv. Phys.* **32**, 791 (1983), and references therein.

²¹W. Werfelmeier, *Z. Phys.* **107**, 332 (1937).

²²W. Andreoni and G. Pastore (unpublished).

²³K. Raghavachari and C. M. Rohlfing, *Chem. Phys. Lett.* **143**, 428 (1988).

²⁴L. A. Bloomfield, R. R. Freeman, and W. L. Brown, *Phys. Rev. Lett.* **54**, 2246 (1985); Q.-L. Zhang, Y. Liu, R. F. Curl, F. K. Tittel, and R. E. Smalley, *J. Chem. Phys.* **88**, 1670 (1988).